Journal Pre-proof

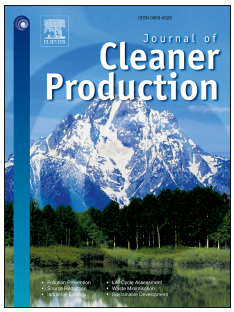

Regulating the ion migration pathways to enhance Joule heating effect and dense nonaqueous phase liquid removal using pulsed direct current

Di Zheng, Zhen Qi, Zhuning Geng, Wan Huang, Guanghe Li, Fang Zhang

PII: S0959-6526(25)00936-9

DOI: https://doi.org/10.1016/j.jclepro.2025.145586

Reference: JCLP 145586

To appear in: *Journal of Cleaner Production*

Received Date: 18 October 2024

Revised Date: 20 April 2025

Accepted Date: 23 April 2025

Please cite this article as: Zheng D, Qi Z, Geng Z, Huang W, Li G, Zhang F, Regulating the ion migration pathways to enhance Joule heating effect and dense nonaqueous phase liquid removal using pulsed direct current, *Journal of Cleaner Production*, https://doi.org/10.1016/j.jclepro.2025.145586.

This is a PDF file of an article that has undergone enhancements after acceptance, such as the addition of a cover page and metadata, and formatting for readability, but it is not yet the definitive version of record. This version will undergo additional copyediting, typesetting and review before it is published in its final form, but we are providing this version to give early visibility of the article. Please note that, during the production process, errors may be discovered which could affect the content, and all legal disclaimers that apply to the journal pertain.

© 2025 Published by Elsevier Ltd.

Graphical abstract

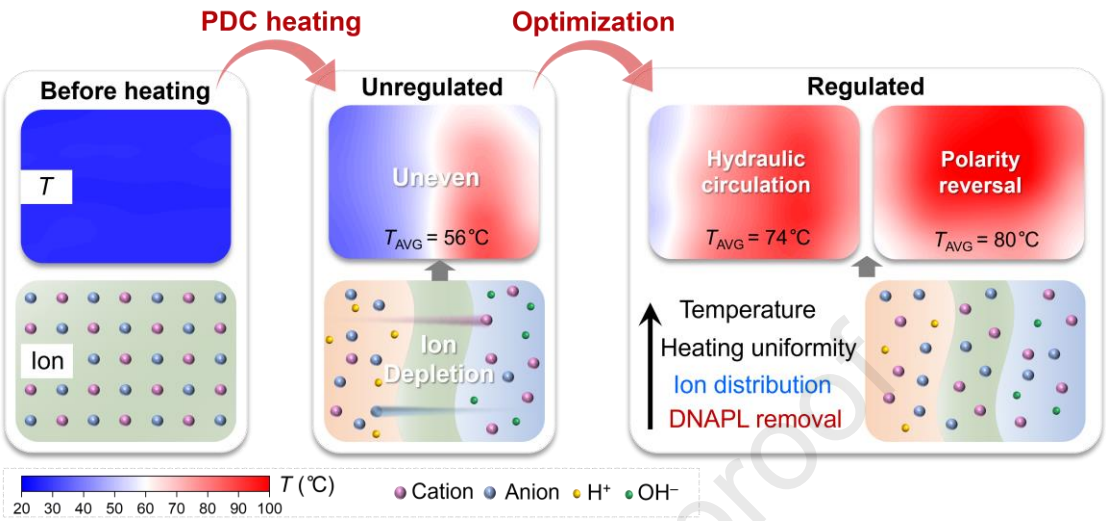

Journal Pre-proof

Journal Pre-proof

Regulating the ion migration pathways to enhance Joule heating effect and dense nonaqueous phase liquid removal using pulsed direct current

Di Zheng [a], Zhen Qi [a], Zhuning Geng [a], Wan Huang [a], Guanghe Li [a, b], Fang Zhang [a,b,*]

[a] School of Environment, State Key Laboratory of Regional Environment and Sustainability, Tsinghua University, Beijing 100084, PR China

[b] National Engineering Laboratory for Site Remediation Technologies (NEL-SRT), Beijing 100015, PR China

* Correspondence: Dr. Fang Zhang

Tel.: 8610 62789655;

Fax: 8610 62785687;

E-mail: fangzhang@tsinghua.edu.cn

Wordcount: 6762 words

Journal Pre-proof

Journal Pre-proof

Abstract

Electrical resistance heating (ERH) based on pulsed direct current (PDC) is a novel and promising *in-situ* technology for the remediation of dense nonaqueous phase liquid (DNAPL) contaminated sites. However, the uniformity and stability of heating still require further improvement. In this study, we proposed an effective strategy for optimizing the PDC heating process by regulating the ion behavior within porous media. Hydraulic circulation (flow field control) and intermittent polarity reversal (electric field control) were introduced as regulation measures for ion behavior, leading to overall improvements in average temperature, heating uniformity, EC and ion distribution uniformity, DNAPL removal, and energy efficiency. Compared to the unregulated system, heating uniformity improved significantly, with approximately a 40% reduction in the coefficient of variation and a 15–30°C increase in the average temperature. The uniformity of ion and EC distribution was significantly enhanced, while severe local ion depletion was effectively prevented, demonstrating the importance of regulating ion migration pathways. Following these regulatory measures, chlorobenzene DNAPL removal efficiency increased by 19.8%–37.8%, while energy consumption decreased by 12.8%–47.5%. These findings suggest that regulating the ion migration pathways was a promising approach for optimizating thermal remediation using PDC.

Keywords: Groundwater remediation; Thermal remediation; Dense nonaqueous phase liquids; Ion migration; Chlorobenzene.

Journal Pre-proof

1. Introduction

Soil and groundwater contamination by dense nonaqueous phase liquids (DNAPLs), such as chlorinated solvents and creosote, has emerged as a pervasive and severe environmental issue in numerous industrialized countries [1-5]. *In-situ* thermal remediation is a competitive solution for DNAPL pollution remediation at such sites owing to its effectiveness in overcoming mass transfer limitations in soil permeability and improving remediation efficiency [6-9]. Electrical resistance heating (ERH) is one of the most frequently used thermal remediation technologies [6, 10-13]. It was typically applied by inputting high-output alternating current (AC) to subsurface porous media, where electrical energy is converted to heat based on Joule's Law [14-16].

Pulsed direct current (PDC) offered a recent alternative to conventional AC for ERH, effectively integrating electrokinetic-driven migration with the Joule heating effect [17-20]. ERH using PDC (PDC-ERH) has shown advantages over AC-ERH, including faster heating rates, lower energy consumption, and stronger pollutant driving effects in low permeability zones [17-20]. The PDC-ERH system was first proposed in 2021 and applied to the removal of trichloroethylene DNAPL, achieving faster heating and approximately 30% lower energy consumption compared to AC-ERH [19]. Subsequently, studies revealed that PDC-ERH enhanced the migration of nitrobenzene DNAPL at sub-boiling temperature compared to AC, consequently improving contaminant accessibility in porous media [18]. Furthermore, PDC-induced thermal activation of persulfate significantly improved the degradation of polycyclic aromatic hydrocarbons compared to AC [17]. A recent study has further elucidated the

Journal Pre-proof

enhancement mechanisms and dynamic effects of Joule heating on electrokinetic transport processes [21]. These encouraging findings underscore the potential of PDC-ERH as a promising *in-situ* remediation technology.

Nevertheless, a lingering concern with PDC-ERH was the uneven temperature distribution with significant spatiotemporal variations during the heating process [22]. In contrast to traditional AC-ERH, where the electric field direction periodically alternates at 50 or 60 Hz [7], causing minimal impact on ion distribution and stable temperature, PDC maintains a constant electric field direction, triggering electrokinetically driven ion migration and thereby creating more complex effects on media conductivity and temperature [22]. In some case, the average temperature of the media may even decrease after a period of heating [19, 22]. These issues hinder continuous and uniform remediation, requiring further investigation and solution. Our prior research revealed that the uneven temperature distribution and great spatiotemporal variations were primarily caused by dynamic ion behaviors, involving complex interplays among reactions, electrokinetic-driven migration, and mixed convection during the heating process [22]. During the heating process, the potential gradient in the local media region significantly increased, eventually leading to severe local ion depletion (up to 99%), resulting in current and temperature drop, as well as uneven heat distribution [22]. Similar ion effects have also been observed in some studies on electrokinetic removal of inorganic contaminants [23, 24]. To address the aforementioned issues with PDC-ERH, incorporating effective regulation of ion behaviors to mitigate severe ion depletion may be a viable strategy.

PDC-ERH is a typical coupling process that involves interactions among electric field, flow field, temperature field, and hydrochemical field. Controlling the flow and electric fields has the potential to directly influence ion migration pathways, thereby impacting the hydrochemical and temperature fields while optimizing the heating remediation process. Some studies on direct current electrokinetic remediation have employed hydraulic circulation and electrode polarity reversal to enhance the distribution of inorganic nutrients, regenerate electroosmotic flow [25-27], and intensify pollutant removal [28, 29]. Our previous research also preliminarily introduced groundwater circulation to enhance the removal of dissolved nitrobenzene in the low permeability zone using PDC [20]. However, the detailed regulation mechanisms of these measures on spatiotemporal temperature changes in the porous media and their subsequent effects on DNAPL removal still require further understanding.

In this study, we introduced hydraulic circulation (flow field control) and intermittent electrode polarity reversal (electric field control) to optimize the heating performance and DNAPL removal of PDC-ERH while maintaining a constant electric field intensity. Chlorobenzene (CB), a typical chlorinated solvent, was used as the model DNAPL contaminant due to its extensive industrial use, high detection frequency, resistance to degradation, and high toxicity [30-34]. We compared the spatiotemporal evolution of media temperature, DNAPL removal, and energy consumption across three heating systems: the unregulated PDC heating system (PDCH), hydraulic circulation enhanced PDC heating system (HCE-PDCH), and polarity reversal enhanced PDC

heating system (PRE-PDCH). To further investigate key regulation mechanisms, we also systematically analyzed the evolution of electrical conductivity (EC) and major ion composition of pore water and porous media, as well as electrical signals during heating.

2. Materials and methods

2.1 Experimental setup

Heating experiments were conducted in a custom-built two-dimensional (2D) sandbox with internal dimensions of 54 cm × 30 cm × 4.5 cm, schematically illustrated in Fig. 1. The heating experimental system comprised the main sandbox, power supply, fluid delivery, and monitoring modules. Silica sand (40/60 mesh, Shanghai Macklin Biochemical Co., Ltd) and kaolin (Sinopharm Chemical Reagent Beijing Co., Ltd) were used to simulate high permeability (~2.5×10^{-2} cm s^{-1}) and low permeability (~3.7×10^{-7} cm s^{-1}) zones. The dimensions of the low permeability lens were 27 cm × 13 cm × 4.5 cm. This heating system and heterogeneity model have been applied in our prior study [18, 22]. More detailed information about the experimental setup and media packing can be found in these previous publication.

Journal Pre-proof

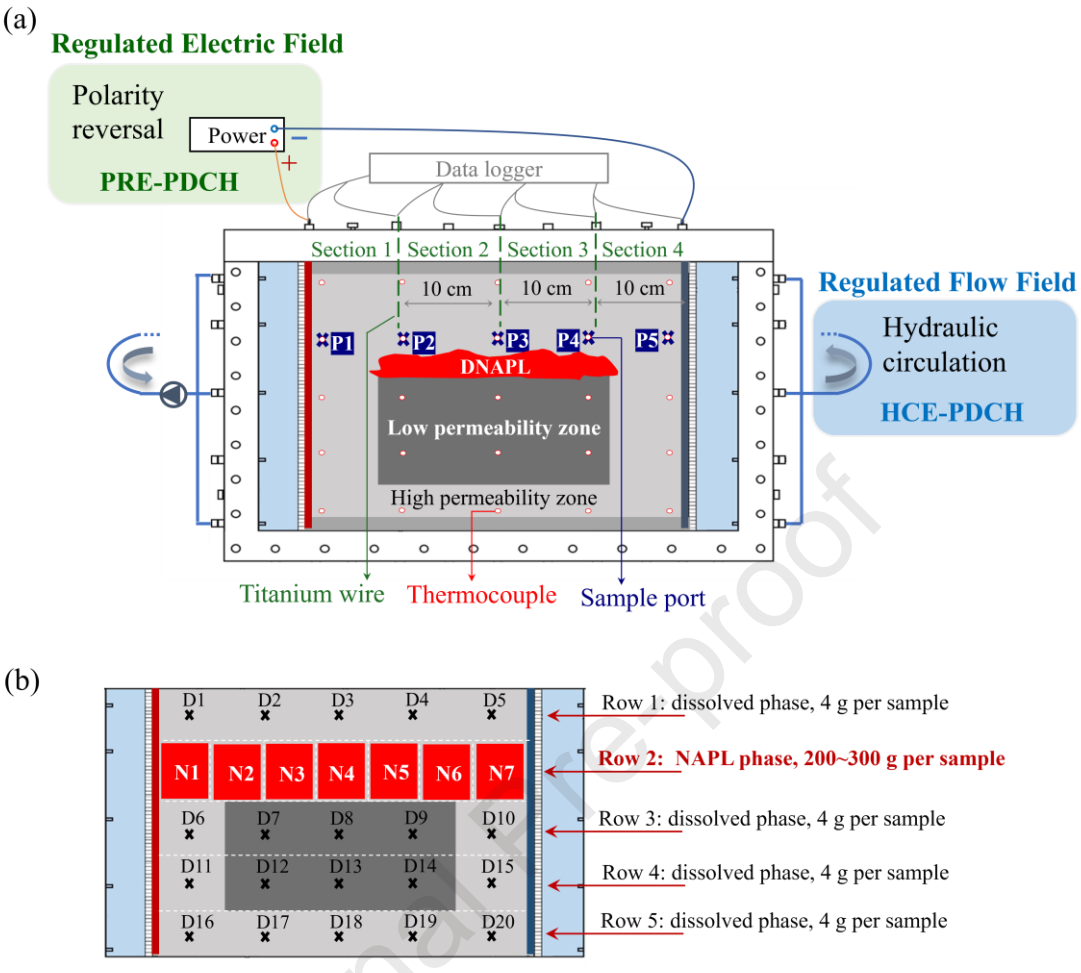

Fig. 1 Schematic diagram of the experimental setup. (a) Schematic diagram of the treatment system, (b) details of sampling points distribution.

Thermocouples (arranged in 5 rows and 5 columns, 4 mm in diameter, K-type, Cesmooy, China) were installed on the back plate and connected to the data acquisition system (Agilent 34970A) to record the temperature of porous media. Meanwhile, five sampling ports (Fig. 1, P1–P5) were installed for collecting pore water samples. Sampling ports P1-P5 were located 2, 11, 20, 29, and 38 cm away from the anode, respectively. To indirectly assess the variations in EC of different media zones, three embedded titanium wires horizontally divided the whole porous media zone into four sections for measuring the partial voltage of each zone.

Journal Pre-proof

135

136 **2.2 Experimental operations**

137 Table S1 summarizes all experimental conditions. To illustrate the enhanced
138 heating effects and mechanisms of hydraulic circulation and polarity reversal on PDC
139 heating, we first conducted HCE-PDCH and PRE-PDCH experiments without DNAPL,
140 and compared it with the previous unregulated PDCH system (Exp.1-Exp.3). In the
141 HCE-PDCH experiment, fluids were peristaltically pumped from the cathode chamber
142 to the anode chamber at the flow velocity of 5.4 mL min^{-1} (pore velocity ~ 0.6 m d^{-1})
143 to simulate the groundwater circulation. For the PRE-PDCH experiment, input electric
144 field conditions were programmed using a programmable power supply, with a fixed
145 interval set for automatic electrode polarity reversal. Based on observations from our
146 previous unregulated PDCH experiment, where a decline in media temperature
147 occurred after approximately 6 h, we selected a polarity reversal interval of 6 h. That is,
148 the positive and negative poles of the power supply automatically switched every 6 h.
149 These experiments lasted for 48 h.

150 Except for the control measures, all other experimental conditions were
151 completely consistent with the unregulated PDCH experiment. All experiments were
152 performed at room temperature and applied a same voltage gradient of 3 V cm^{-1} (120
153 V). The bulk solution was 0.02 M Na_2SO_4 solution. In the PDCH and PRE-PDCH
154 experiments, fluids were pumped into the left anolyte chamber through three inlets at a
155 flow velocity of 1.6 mL min^{-1} (~0.2 m d^{-1}) to simulate natural groundwater flow. The
156 pumped fluids were identical to the initial bulk solution.

Journal Pre-proof

To evaluate the heating performance, the temperature of porous media was continuously monitored with intervals of 1 min. To further elucidate the influence mechanism of the regulation measures, the system current was automatically recorded every second using the programmable power supply, while the partial voltages in distinct media zones were determined every minute using the data acquisition system to continuously reflect the relative variations in EC of these zones. Simultaneously, pore water was regularly collected from sampling ports (P1–P5) at 0 h, 12 h, 24 h, 36 h, and 48 h. Following the heating experiment, the media were sampled in 5 rows and 6 columns. These samples were then used to analyze the physicochemical properties, including pH, EC, and concentrations of main water-soluble ions (sulfate and sodium ions).

To further assess the DNAPL removal and energy consumption, we also performed three DNAPL removal experiments using PDCH, HCE-PDCH, and PRE-PDCH (Exp.4-Exp.6). The Oil Red O dyed CB DNAPL (20 mL, 22 g) was pre-added above the low permeability lens, as shown in Fig. 1a, while a photograph of the actual sandbox packed with the porous media and CB DNPAL was provided in Fig. S1. Oil Red O ($C_{26}H_{24}N_4O$) is a lipophilic, non-ionic dye that was used in our study specifically for the visualization of DNAPL [35-38]. The media sample was collected after 24 h to analyze residual CB concentration and mass. Details of sampling points distribution was shown in Fig. 1b. The porous media were sampled in 5 rows. Since nearly all of the NAPL-phase contaminants were concentrated in the second row, this row was divided into 7 sections (N1-N7). The media in these seven sections were completely

Journal Pre-proof

collected and weighed, with each sample weighing approximately 200–300 g. In other zones, the contaminants were present in the dissolved phase. We divided these zones into 20 parts and sampled at the center of each part (D1-D20). Water samples from the electrode chambers were also fully collected. Meanwhile, the current was recorded to calculate energy consumption.

2.3 Analyses and calculations

The determination method of media specimens referred to EPA 9045D (2004) for saturated soil. Four grams of wet media were weighed and added to 10 mL of ultrapure water, and the supernatant was analyzed after thorough shaking. The EC and pH of the collected aqueous samples were determined using a multiparameter meter (Seven Excellence, Mettler Toledo) equipped with both an EC micro-electrode (InLab 751, 4 mm diameter) and a pH micro-electrode (InLab Micro, 3 mm diameter). Sodium and sulfate ion concentrations were measured using ion chromatography (ICS 2000, Dionex). The determination of sodium ion involved a cation-exchange column (IonPac CS12A, Dionex) with a 20% methanesulfonic acid solution as the eluent and a flow rate of 1 mL min^{-1}. Sulfate ions were determined using an anion exchange column (IonPac AS11-HC, Dionex) with the eluent (30 mM KaOH) at a flow rate of 1.2 mL min^{-1}.

The coefficient of variation (CV) was used to describe the uniformity degree of temperature and EC distribution in porous media.

$$CV = \frac{\text{standard deviation}}{\text{average value}} \quad (1)$$

198 The electromigration velocitiy ($u_{\mathrm{mig},i}$, m s^{-1}) of ions in porous media during PDC
199 heating was derived from Eq. (2):

$$u_{\mathrm{mig},i} = -D_i \frac{z_i F}{RT} \nabla \Phi \quad (2)$$

200 in which D_i [m^2 s^{-1}] is the effective diffusion coefficient for porous media, z_i is the
201 charge number, $\nabla\Phi$ [V m^{-1}] is the electric potential; F is the Faraday constant, R is
202 the gas constant, T [K] is the temperature. More details can be found in our previous
203 paper [22].

204 The CB concentration was measured by GC-MS (Agilent 7980A-5975). Each
205 media sample was mixed with 0.1 mol L^{-1} H_2SO_4 and hexane. Based on the sample
206 weight, CB was extracted from the media using a ratio of 1 g wet soil : 1 mL H_2SO_4 :
207 2.5 mL hexane. The total CB removal efficiency (φ, %) after 24 h was calculated
208 according to Eq. (3).

$$\varphi = \frac{m_{\mathrm{water}} + m_{\mathrm{soil}}}{m_0} = \frac{c_{\mathrm{water}} V_{\mathrm{water}} + \sum_{i=1}^{i=27} m_i c_i}{m_0} \quad (3)$$

209 where m_{water} [g] is the residual CB mass in electrode chambers, m_{soil} [g] is the residual
210 CB mass in porous media, m_0 [g] is the CB initial mass (~ 22 g), c_{water} [g L^{-1}] is the CB
211 concentration in electrode chamber solution, V_{water} [L] is the volume of electrode
212 chamber solution (~2 L), c_i [g g^{-1} wet soil] is the CB concentration in porous media
213 (N1-N7, D1-D20), m_i [g] is the meida weight corresponding to each region.

214 The energy consumption per log CB removal (W, kWh $\log^{-1}$) was calculated by Eq.
215 (4):

Journal Pre-proof

$$W = \int_0^t UI\mathrm{d}t \times \left[\log \frac{m_0}{m_t} \right]^{-1} \quad (4)$$

where U [V] is the input voltage, I the current [A] is recorded by data acquisition every 1 min, t [h] is the reaction time, m_t [g] is the total residual CB mass after 24 h, m_0 [g] is the CB initial mass (~ 22 g).

3. Results and discussion

3.1 Improved heating performance: average temperature and uniformity

We compared the spatiotemporal temperature evolution in PDC heating systems using different regulation measures (Exp.1-Exp.3). The results showed that introducing hydraulic circulation or intermittent polarity reversal significantly improved the heating performance of PDC (Fig. 2). In the case without additional regulation measures (i.e., PDCH system), the average temperature experienced a rapid increase over the first 6 h, followed by a drop, and then a slight rebound at 36 h (Fig. 2a). After 48 h, the average temperature remained at only 60°C. In contrast, the HCE-PDCH system maintained a relatively stable average temperature after peaking, ranging from 71~75°C. Meanwhile, the PRE-PDCH system showed a higher average temperature of 75~83°C after peaking, with periodic fluctuations occurring every 6 h following polarity reversal. These regulatory measures prevented a continuous drop in temperature and further elevated the average temperature by 15~30°C compared to the unregulated system.

Journal Pre-proof

Following the implementation of these regulatory measures, the uniformity of temperature distribution also improved significantly. To quantify this improvement, we calculated the temperature coefficient of variation, which served as an indicator of heating uniformity. A lower coefficient of variation indicates a more uniform spatial distribution of temperature [39]. Compared to the PDCH system, the temperature coefficient of variation for both the HCE-PDCH and PRE-PDCH systems decreased by approximately 40% (Fig. 2b), indicating a significant improvement in heating uniformity. Fig. 2c presented the two-dimensional spatial distribution of temperature at 12 h intervals. In contrast to the uneven temperature distribution with significant dynamic changes in the PDCH system, the temperature distribution in both the HCE-PDCH and PRE-PDCH systems became more uniform and relatively stable after peaking at 12 h. During the HCE-PDCH experiment, although heating uniformity improved, the temperature on the anode side (near the pump inlets) remained lower than in other zones, likely due to the cooling effect of the hydraulic circulation process. In the PRE-PDCH system, the temperature distribution showed an almost axisymmetric pattern.

Journal Pre-proof

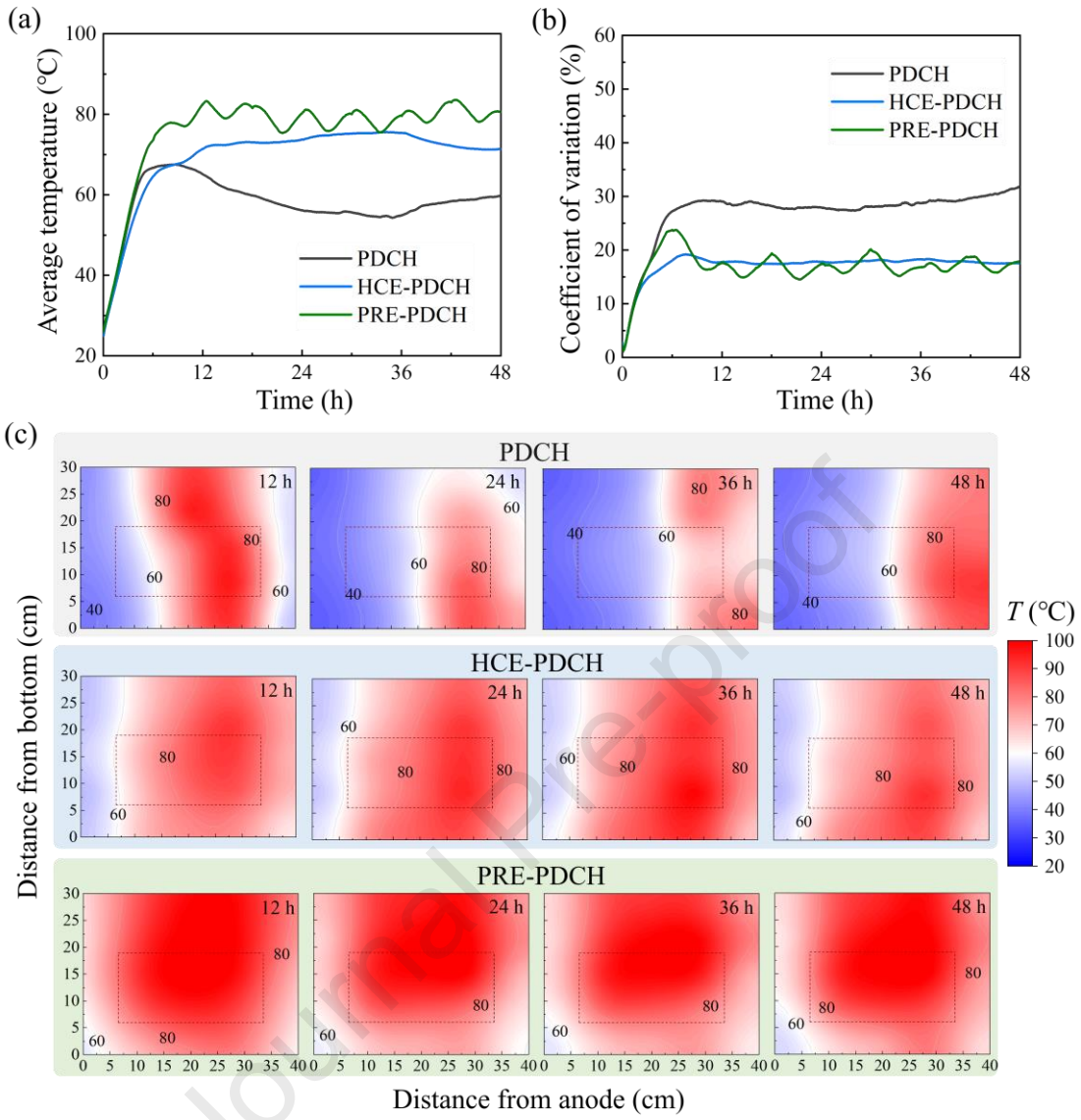

Fig. 2 Variations in (a) average temperature, (b) temperature coefficient of variation, and (c) two-dimensional spatial distribution of temperature over time in three systems: PDCH (unregulated PDC heating system), HCE-PDCH (hydraulic circulation enhanced PDC heating system), and PRE-PDCH (polarity reversal enhanced PDC heating system). The dashed frame area represented the kaolin lens.

Journal Pre-proof

Journal Pre-proof

3.2 The key enhanced mechanism: optimizing ion migration and distribution

According to the Joule's law, temperature evolution was directly related to current and partial resistance. Our prior study revealed that the uneven temperature distribution and significant spatiotemporal variations during PDC heating primarily stemmed from dynamic ion behaviors with the impact of multi-fields including electric field, flow field, and thermal field, etc [22]. Notably, severe local ion depletion led to drops in current and temperature during the heating process [22, 40, 41]. In this study, the observed improvements in heating performance may be likely attributed to the effective regulation of ion migration pathways. This section discussed and elucidated the detailed mechanisms involved.

3.2.1 Variations in electrical signals and ionic composition of pore water among the direction of electric field

We first recorded real-time current in different systems. To evaluate changes in partial resistance, partial voltages across different media regions were monitored to indirectly assess variations in media resistance, while the EC and ionic composition of pore water among the direction of electric field was also directly measured.

Similar to the average temperature trends (Fig. 2a), hydraulic circulation and intermittent polarity reversal effectively suppressed the current drop during the PDC heating process, with stabilized current values increasing by 25~63% compared to the unregulated system (Fig. 3a). In the HCE-PDCH system, the current initially increased at a slightly slower rate than in the PDCH system but gradually stabilized at a higher

value of ~1.2 A. In the PRE-PDCH system, the initial behavior resembled that of the PDCH system, showing a notable decrease in current between 3~4 h. However, the current rapidly elevated after the first polarity reversal at 6 h, with subsequent reversals causing significant current surges. Two polarity reversals constituted one heating cycle and triggered periodic changes in both current and temperature, demonstrating the key role of polarity reversal in regulating current and temperature during the PDC heating process.

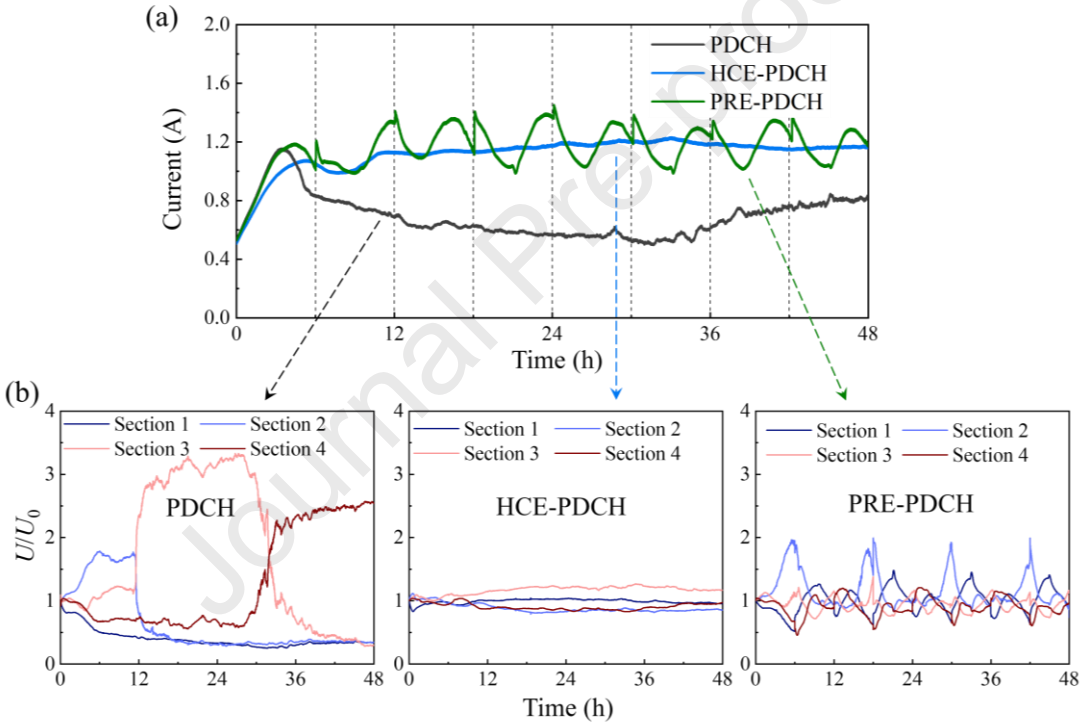

Fig. 3 Variations in system electrical signals over time. (a) system current and (b) media partial voltage, where U/U_0 is the ratio of real-time partial voltage to initial partial voltage in the different media sections. The media zone was equally divided into four sections along the direction of the electric field to measure the partial voltage, with sections 1 to 4 ranging from left to right within the sandbox.

289 Analysis of partial voltage and pore water EC jointly showed a significant
290 improvement in the spatial uniformity of EC distribution for both the HCE-PDCH and
291 PRE-PDCH systems compared to the PDCH system (Fig. 3b and Fig. 4). In contrast to
292 the PDCH system, where local partial voltage increased to 2~3 times their initial value,
293 the variations in partial voltage in different media sections during HCE-PDCH
294 remained within 27% of the initial value. Additionally, the EC range for pore water
295 samples (measured at 12 h, 24 h, 36 h, and 48 h) was 5.5~9.2 mS cm^{-1} in the HCE-
296 PDCH system, much narrower than the range of 0.293~26.0 mS cm^{-1} observed in the
297 PDCH system (Fig. 3). The initial pore water EC was ~4 mS cm^{-1}. Therefore, no
298 significant decline in EC was observed during the HCE-PDCH process. Since the EC
299 is the index of water-soluble ions content [24], these results suggest that hydraulic
300 circulation might effectively avoid severe ion depletion that has been previously proven
301 to cause drops in both current and temperature during PDCH.

Journal Pre-proof

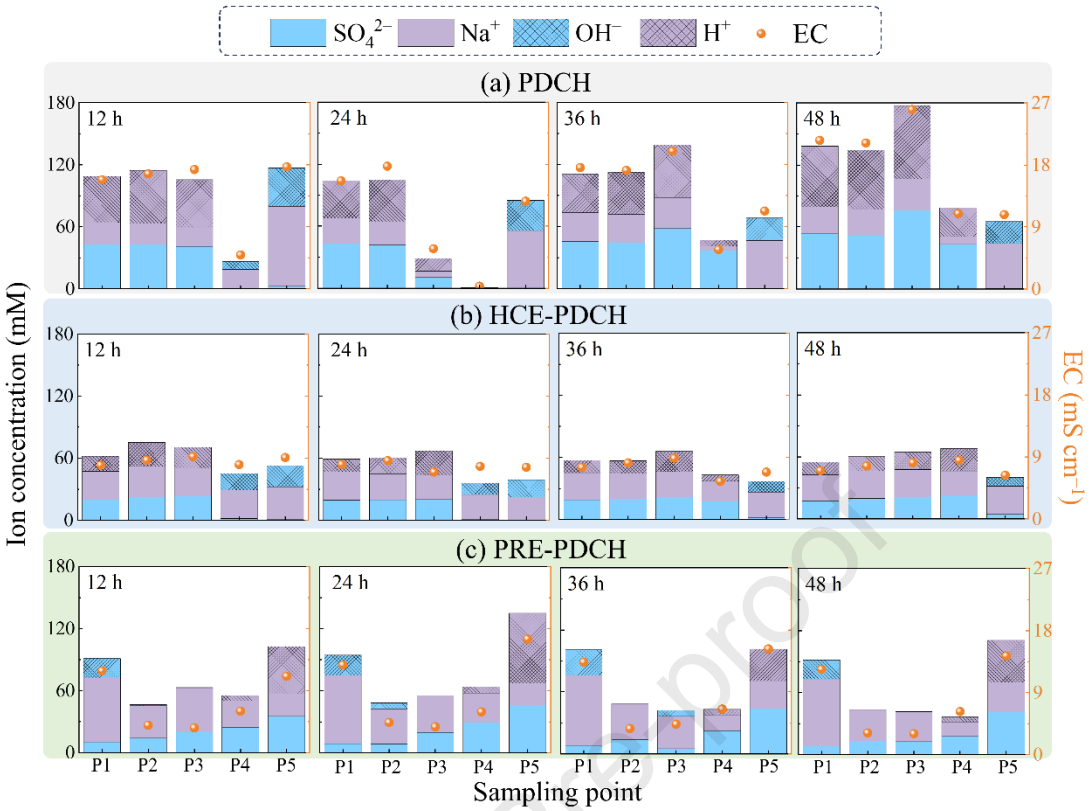

Fig. 4 EC and main ion concentration (Na^+, H^+, SO_4^{2-} and OH^-) distribution along the direction of input electric field. Samples P1-P5 were pore water withdrawn from sampling points of 2, 11, 20, 29, and 38 cm away from the left electrode.

Although hydraulic circulation homogenized the EC distribution, further detailed analysis of ion composition in pore water (Fig. 4b) still revealed significant changes compared to the initial composition of 20 mM Na_2SO_4 during HCE-PDCH. In the unregulated PDCH system, a clear pH jump was obsevered, which indicated that the acidic and alkaline fronts of groundwater met in the media [22, 40]. In this HCE-PDCH system, acidic, pH jump, and alkaline zones still gradually formed due to continuous water electrolysis, yet severe ion depletion did not occur in the pH jumping zone. For example, the pH jumping zone in the third section of the media at 12 h exhibited only a 15% increase in partial voltage from the initial value, in contrast to a surge exceeding

315 300% observed with severe ion depletion in the PDCH system (Fig. 3b). Additionally,
316 concentrations of H^+ and OH^- in pore water during HCE-PDCH were significantly
317 lower than those in the PDCH system (Fig. 4a), owing to the circulation of cathode
318 effluent into the anode well. Some H^+ and OH^- neutralized in the anode well,
319 contributing to the enhanced uniformity of EC and potential gradient.

320 Regarding stable water-soluble ions, Na^+ showed a relatively uniform distribution
321 with a concentration range of 20 mM~40 mM (Fig. 4b), likely attributed to circulation
322 facilitating the delivery of Na^+ from the cathode to the anode. Based on parameters
323 under stable temperature conditions (72°C), the ion electromigration velocity of Na^+
324 was estimated to be 2.3×10^{-5} m s^{-1}, consistent with the groundwater flow velocity,
325 supporting the relatively stable migration of Na^+ within porous media. The uniform
326 distribution of Na^+ further enhanced the uniformity of EC and potential gradient. For
327 SO_4^{2-}, the concentration continued to decrease significantly after 12 h (< 1 mM) in the
328 alkaline region. This decrease was attributed to the electromigration of SO_4^{2-} towards
329 the anode opposing the direction of groundwater flow. Nevertheless, the presence of
330 Na^+ and OH^- prevented a significant decline in the EC of the alkaline region. Pore water
331 samples with a near-neutral pH were not directly collected during HCE-PDCH.
332 However, according to the electroneutrality theory, if Na^+ were found in the near-neutral
333 zone, an equally charged amount of anions (i.e., SO_4^{2-}) would be required [42]. These
334 findings indicate that maintaining a relatively uniform distribution of one stable water-
335 soluble ion would be effective when regulating ion behavior to prevent severe ion
336 depletion and consequent declines in temperature and current.

Journal Pre-proof

Regarding the PRE-PDCH system, with periodic changes in the direction of the input electric field, pore water EC and ion composition, as well as media partial voltage also exhibited corresponding periodic variations (Fig. 3c and Fig. 4c). The electrode polarity automatically reversed every 6 h, forming a cycle of each 12 h. In the initial 6 h, the media partial voltage was similar to that of the PDCH system (Fig. 3a). The partial voltage in the second section of media gradually increased, with a maximum amplitude close to 100%, thus leading to a decrease in current after 4 h (Fig. 2). Following a 6-hour electrode polarity reversal, the above partial voltage declined, and simultaneously, the current rapidly increased. At 12 h, the media partial voltage became uniform with a change in amplitude from the initial value of only 6~14%. During the subsequent polarity transition cycle, the partial voltage exhibited a similar periodic change, with the highest partial voltage change amplitude always less than 100%, lower than the maximum increase of 300% in the unregulated case.

Variations in EC and ion composition of pore water also followed a periodic pattern. At 6 h, the pH jump zone initially showed a significant decrease in ion concentration and EC, yet gradually returned to levels close to the initial conditions at 9 h (i.e., 3 h after the first polarity reversal), as depicted in Fig. S2. The above changes can be attributed to the reversal of ion electromigration direction with the shift of electrode polarity, thereby improving the uniformity of ion distribution. Subsequently, a similar EC and ion distribution was observed at the end of each polarity transition cycle (i.e., 12 h, 24 h, 36 h, and 48 h, Fig. 4c). The detected ion concentration range was 14~66 mM for Na^+ and 8~46 mM for SO_4^{2-}. We collected a pore water sample near

Journal Pre-proof

359 the pH jumping zone at 24 h (P3, pH = 8.36), where the concentrations of Na^+ and
360 SO_4^{2-} remained close to their initial values, providing direct evidence that the
361 regulatory measures of intermittent polarity reversal effectively prevented ion depletion
362 in the pH jumping zone.

363 3.2.2 Changes in physicochemical properties after heating

364 In order to gain a deeper understanding of the spatial variation in media properties, the
365 pH, EC, and major ions of media were analyzed after 48 h of heating. The media zone
366 was divided equally into 30 parts in 6 rows and 5 rows after the experiment. The EC
367 and ion concentration results of these media samples were provided in Fig. S3, while
368 the corresponding two-dimensional spatial distribution in different heating systems was
369 plotted in Fig. 5. Similar to the results of pore water, the uniformity of EC, Na^+, and
370 SO_4^{2-} distribution significantly improved with HCE-PDCH and PRE-PDCH compared
371 to PDCH. The maximum difference of EC in different media regions was only 1.6 mS
372 cm^{-1} for HCE-PDCH and 1.5 mS cm^{-1} for PRE-PDCH, whereas the difference using
373 PDCH (7.1 mS cm^{-1}) was 4~5 times that of these regulated systems (Fig. S3). The EC
374 coefficient of variation decreased from 0.75 in the PDCH system to 0.40 in the HCE-
375 PDCH system and 0.47 in the PRE-PDCH system (Fig. S4).

Journal Pre-proof

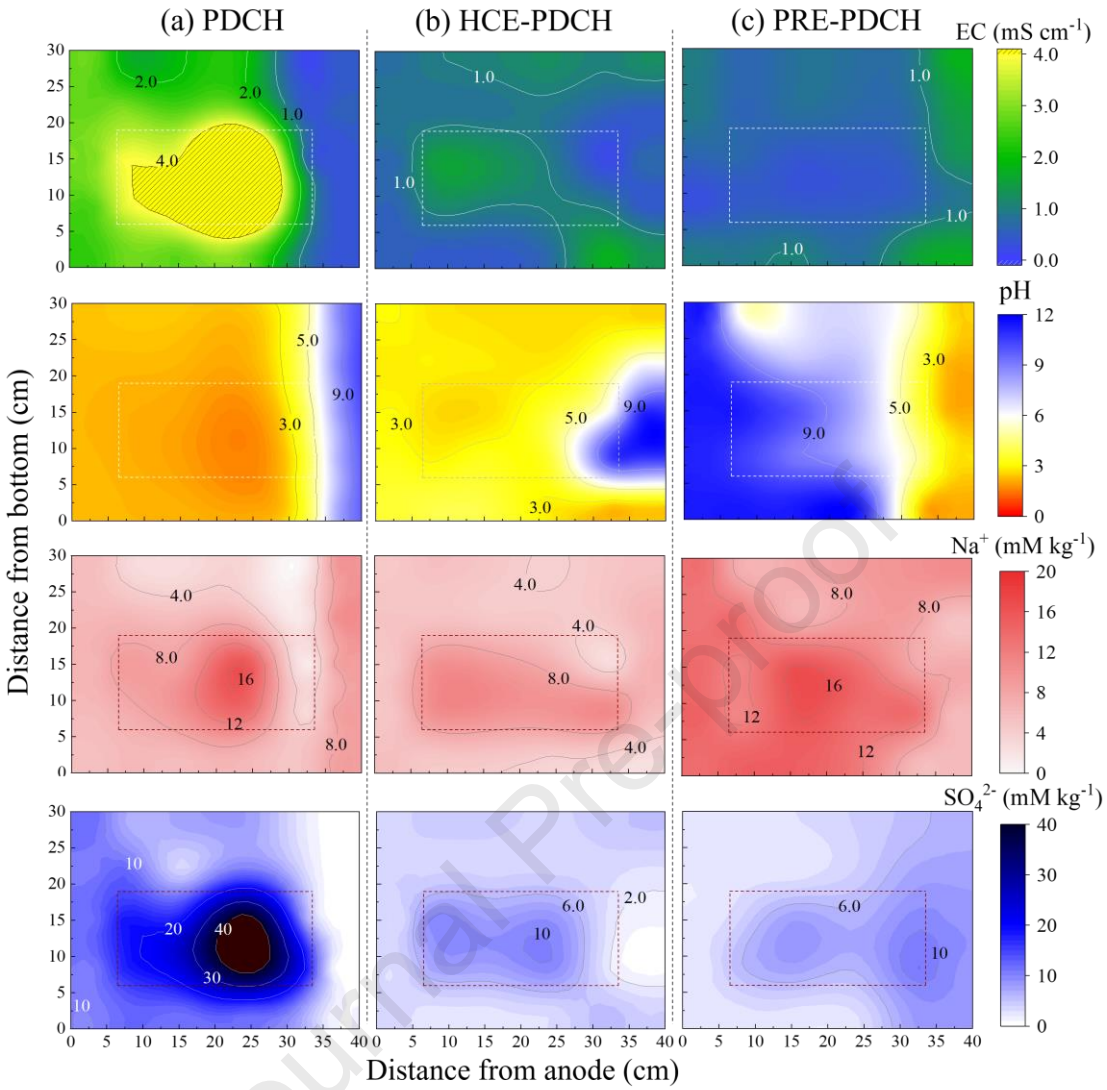

Fig. 5 Two-dimensional spatial variations in physicochemical properties of porous media after 48 h.

In terms of the two-dimensional spatial distribution, the downstream of the low-permeability lens still showed a significant decrease in EC and ion concentration in the HCE-PDCH system (Fig. 5b). The EC value and ion concentrations were reduced by more than 60% from the initial value. This phenomenon indicated that regulating ion transport downstream of the lens was challenging owing to the flow bypassing. Nevertheless, effective regulation for ion and EC distribution across other high

permeability zones could establish efficient current paths, thus having relatively little impact on the overall current and temperature of the system.

With PRE-PDCH, the concentrations of Na^+ and SO_4^{2-}, as well as EC at all sampling points remained at high levels (Fig. 5c). Multiple sampling samples from both high permeability and low permeability media zones were collected in the pH jumping zone with pH values ranging from 5 to 9. These results once again confirmed that polarity reversal can effectively regulate ion migration and prevent severe ion depletion within the pH jumping zone. In addition, a comparative analysis of ion concentrations showed that the Na^+ concentration using PRE-PDCH was approximately twice that using HCE-PDCH. This difference was likely attributed to the migration direction of Na^+ towards the upstream during the previous 6 h (42~48 h), resulting in more Na^+ being trapped in the porous media driven by electric field forces.

3.3 Enhanced DNAPL removal and energy efficiency

We selected CB DNAPL as a model pollutant and further compared CB removal in the PDCH, HCE-PDCH, and PRE-PDCH systems (Exp.4-Exp.6). Residual CB concentration distribution in porous media after 24 h of heating was shown in Fig. 6a. The residual concentrations in the HCE-PDCH system (< 6.9 mg g^{-1}) and the PRE-PDCH system (< 3.3 mg g^{-1}) were significantly lower than those in the PDCH system (< 11.0 mg g^{-1}). In the PRE-PDCH system, the removal efficiency was the highest at 92.0%, while the HCE-PDCH system achieved a removal efficiency of 74.0% (Fig. 6b). These efficiencies represented a 37.8% and 19.8% improvement compared to the

406 PDCH system (54.2%) at the same voltage gradient. These results indicated that the
407 removal efficiency was positively correlated with heating performance. Furthermore,
408 the co-boiling of NAPL and water is crucial for contaminant removal. Among these
409 systems, the PRE-PDCH system exhibited the highest number of temperature
410 measurement points exceeding the co-boiling temperature (approximately 91°C [43]),
411 along with the longest co-boiling duration, further supporting its superior
412 chlorobenzene removal efficiency.

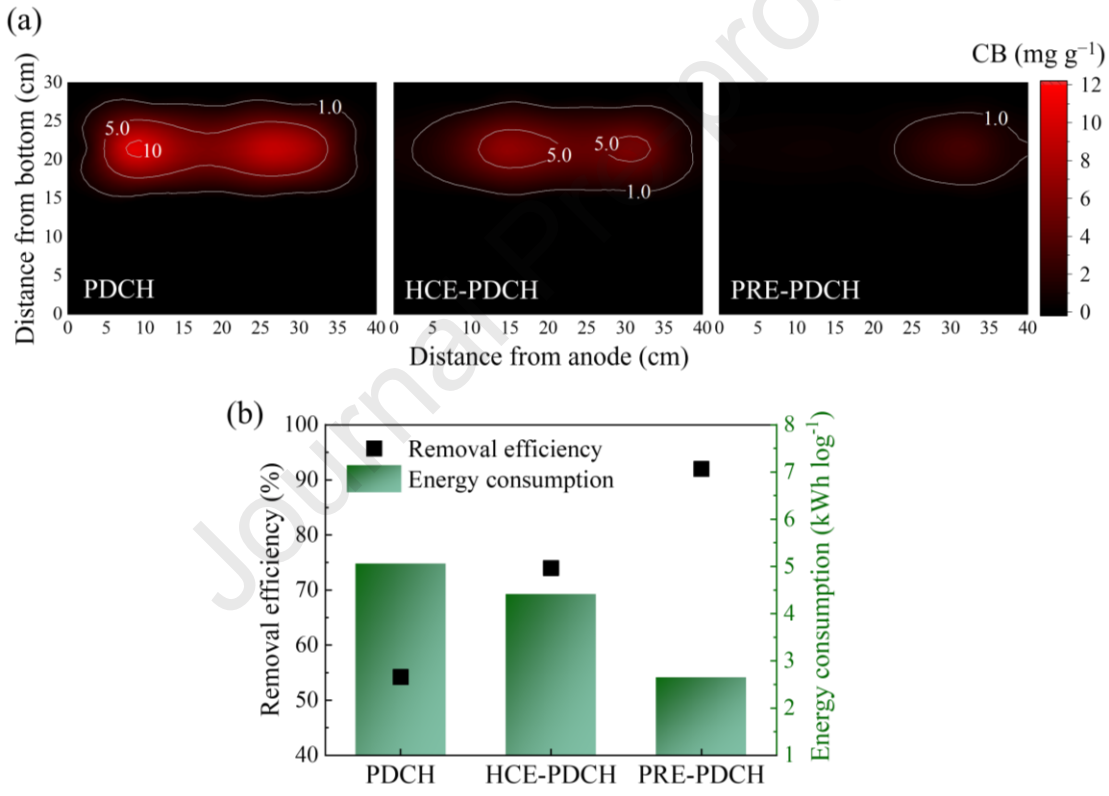

413

414 **Fig. 6** Comparison of (a) residual CB concentration distribution and (b) removal efficiency
415 and energy consumption per log removal after 24 h in different systems.

416 Based on the residual CB mass and current data, the energy consumption per log
417 removal was further calculated for each system (Fig. 6b and Table S2). The PRE-PDCH
418 system achieved the highest DNAPL removal with the lowest energy consumption of

419 2.7 kWh log^{-1}, which was 47.5% lower than that of the PDCH system (5.1 kWh log^{-1}).
420 The energy consumption in HCE-PDCH system (4.4 kWh log^{-1}) was reduced by 12.8%
421 compared to the PDCH system. These comparison results further emphasized the
422 importance of regulating electric and flow fields to ensure continuous and uniform
423 heating of the porous media. With a constant electric field intensity, adjusting the flow
424 or electric field can potentially achieve efficient removal with low energy consumption.
425 Overall, these findings further highlight the potential benefits of PDC-ERH when
426 combined with effective regulation measures, including improved remediation
427 efficiency, reduced energy consumption, and enhanced long-term sustainability. The
428 proposed systems are expected to be applicable to various volatile and semi-volatile
429 contaminants and media conditions, while performance may vary depending on
430 contaminant and media characteristics. Contaminants with high adsorption or low
431 volatility may require additional remediation strategies, such as coupling with other
432 treatment agents [15, 17, 44]. Meanwhile, media permeability and moisture content
433 significantly influence heating uniformity and ion migration [22], especially when
434 groundwater circulation control is employed. In low-permeability formations (e.g.,
435 clay-rich formations), hydraulic circulation may be less effective due to limited fluid
436 flow, while polarity reversal could still enhance ion migration and heating uniformity.
437 Currently, field applications of PDC-ERH remain in the early stages, and our findings
438 would provide a critical foundation for future field implementation. Nonetheless,
439 scaling PDC-ERH for larger applications still presents challenges, particularly the need
440 for precise control over electric and flow fields across heterogeneous sites, which may

Journal Pre-proof

require more complex infrastructure and monitoring systems, potentially leading to higher upfront costs. However, the system's potential for reduced energy consumption and improved efficiency could result in long-term cost savings, while further advancements in automation and real-time monitoring technologies may help mitigate these challenges. Given these considerations, further development and implementation of PDC-ERH in diverse field settings are urgently needed, building on existing AC-ERH practices to fully evaluate the system's scalability and validate its potential advantages.

4. Conclusions

In this study, we demonstrated that introducing external hydraulic circulation and electrode polarity reversal comprehensively enhanced the heating performance (both average temperature and uniformity), uniformity of EC and ion distribution, DNAPL removal, and energy efficiency. Compared to the unregulated heating system at the same voltage, the average temperature of the porous media increased by 15~30°C, while heating uniformity improved markedly with the coefficient of variation decreasing by approximately 40%. Additionally, DNAPL removal efficiency achieved an increase of 19.8%~37.8% with energy consumption decreasing by 12.8%~47.5%. These improvements were primarily attributed to the effective regulation of ion migration pathways in porous media through adjustments to the electric and flow fields. These measures significantly improved the uniformity of ion and EC distribution within the porous media, while effectively preventing pronounced elevations in local electric

Journal Pre-proof

potential gradients and the subsequent formation of severe ion depletion zones. These results showed the importance of effective ion regulation in optimizing PDC heating performance and thereby DNAPL removal. Future work should focus on evaluating the scalability of PDC-ERH in field applications. Additionally, integrating PDC-ERH with complementary remediation methods (e.g., thermally activated persulfate) may further enhance the degradation of recalcitrant contaminants. Developing real-time monitoring systems for ion distribution and temperature gradients will also be essential for optimizing regulation strategies and advancing sustainable remediation.

Acknowledgments

We acknowledge the financial support from the National Natural Science Foundation of China (No. 42077171).

References

[1] A. Guleria, P.K. Gupta, S. Chakma, B.K. Yadav, Unraveling the Fate and Transport of DNAPLs in Heterogeneous Aquifer Systems-A Critical Review and Bibliometric Analysis, Sustainability, 15 (2023) 20.

[2] R.A. Dearden, D.J. Noy, M.R. Lelliott, R. Wilson, G.P. Wealthall, Release of contaminants from a heterogeneously fractured low permeability unit underlying a DNAPL source zone, J. Contam. Hydrol., 153 (2013) 141-155.

[3] X.Y. Xu, N. Hu, Z.K. Qian, Q. Wang, L.W. Fan, X. Song, Understanding of Co-boiling between

Journal Pre-proof

Organic Contaminants and Water during Thermal Remediation: Effects of Nonequilibrium Heat and Mass Transport, Environ. Sci. Technol., 57 (2023) 16043-16052.

[4] H.F. Stroo, A. Leeson, J.A. Marqusee, P.C. Johnson, C.H. Ward, M.C. Kavanaugh, T.C. Sale, C.J. Newell, K.D. Pennell, C.A. Lebrón, M. Unger, Chlorinated Ethene Source Remediation: Lessons Learned, Environ. Sci. Technol., 46 (2012) 6438-6447.

[5] C. Feng, F. Liu, F.Y. Huang, L.P. Chen, E.P. Bi, Dense nonaqueous phase liquids back diffusion controlled by biodegradation and heterogeneous sorption-desorption, Journal of Cleaner Production, 382 (2023) 13.

[6] J. Horst, J. Munholland, P. Hegele, M. Klemmer, J. Gattenby, In Situ Thermal Remediation for Source Areas: Technology Advances and a Review of the Market From 1988-2020, Ground Water Monit. Rem., 41 (2021) 17-31.

[7] D. Ding, X. Song, C. Wei, J. LaChance, A review on the sustainability of thermal treatment for contaminated soils, Environ. Pollut., 253 (2019) 449-463.

[8] F. Kastanek, P. Topka, K. Soukup, Y. Maleterova, K. Demnerova, P. Kastanek, O. Solcova, Remediation of contaminated soils by thermal desorption; effect of benzoyl peroxide addition, Journal of Cleaner Production, 125 (2016) 309-313.

[9] X.Y. Xu, N. Hu, Q. Wang, X.D. Li, Z.T. Yu, X. Song, L.W. Fan, Insights into the Relationship between Temperature Variation and NAPL Removal during In Situ Thermal Remediation of Soil in the Presence of NAPL-Water Co-boiling: A Two-Dimensional Visualized Sandbox Study, Environ. Sci. Technol., 58 (2024) 22594-22602.

[10] A.I.A. Chowdhury, J.I. Gerhard, D. Reynolds, D.M. O'Carroll, Low Permeability Zone Remediation via Oxidant Delivered by Electrokinetics and Activated by Electrical Resistance

Journal Pre-proof

Heating: Proof of Concept, Environ. Sci. Technol., 51 (2017) 13295-13303.

[11] G. Heron, J. Bierschenk, R. Swift, R. Watson, M. Kominek, Thermal DNAPL Source Zone Treatment Impact on a CVOC Plume, Ground Water Monit. Rem., 36 (2016) 26-37.

[12] E.J. Martin, K.G. Mumford, B.H. Kueper, G.A. Siemens, Gas formation in sand and clay during electrical resistance heating, Int. J. Heat Mass Transfer, 110 (2017) 855-862.

[13] Z.S. Yang, C.L. Wei, J. Sima, S. Yan, L.P. Yin, A. Xian, J.Z. Wan, J. Yang, X. Song, Quantitative sustainability assessment for *in-situ* electrical resistance heating coupled with steam enhanced extraction: An effective approach for the development of green remediation technologies, Water Res., 267 (2024) 13.

[14] E.J. Martin, K.G. Mumford, B.H. Kueper, Electrical Resistance Heating of Clay Layers in Water-Saturated Sand, Ground Water Monit. Rem., 36 (2016) 54-61.

[15] X.P. Yue, Y.P. Zhang, Y.P. Shan, K. Shen, W.T. Jiao, Lab-scale transport and activation of peroxydisulfate for phenanthrene degradation in soil: A comprehensive assessment of the remediation process, soil environment and microbial diversity, Sci. Total Environ., 901 (2023) 15.

[16] W.X. Xu, L.F. Cao, R.L. Ge, S.P. Li, Y.X. Wei, Y.F. Yang, G.H. Li, F. Zhang, Long term impact of electrical resistance heating on soil bacterial community based on a field test, Sci. Total Environ., 950 (2024) 9.

[17] D.D. Wen, H.Q. Liu, Y.J. Zhang, R.B. Fu, Electrokinetically-delivered persulfate and pulsed direct current electric field induced transport, mixing and thermally activated in situ for remediation of PAHs contaminated soil, J. Hazard. Mater., 444 (2023) 13.

[18] D. Zheng, Z. Geng, W. Huang, L. Cao, Z. Wan, G. Li, F. Zhang, Enhanced semi-volatile DNAPL accessibility at sub-boiling temperature during electrical resistance heating in

heterogeneous porous media, J. Hazard. Mater., 439 (2022) 129633.

[19] Z. Geng, B. Liu, G. Li, F. Zhang, Enhancing DNAPL removal from low permeability zone using electrical resistance heating with pulsed direct current, J. Hazard. Mater., 413 (2021) 125455.

[20] D. Zheng, Z.N. Geng, R.L. Ge, J.Q. Dong, G.H. Li, F. Zhang, Enhanced migration and degradation of nitrobenzene in heterogeneous porous media using pulsed direct current electrical resistance heating with hydraulic circulation, J. Hazard. Mater. Lett., 5 (2024) 5.

[21] R. Sprocati, A. Gallo, H. Wienkenjohann, M. Rolle, Temperature-dependent dynamics of electrokinetic conservative and reactive transport in porous media: A model-based analysis, J. Contam. Hydrol., 259 (2023) 12.

[22] D. Zheng, Q.L. Xie, F.Z. Li, W. Huang, Z. Qi, J.Q. Dong, G.H. Li, F. Zhang, Spatiotemporal dynamic temperature variation dominated by ion behaviors during groundwater remediation using direct current, Environ. Pollut., 351 (2024) 10.

[23] W.L. Hu, W.C. Cheng, Y.H. Wang, S.J. Wen, Z.F. Xue, Applying a nanocomposite hydrogel electrode to mitigate electrochemical polarization and focusing effect in electrokinetic remediation of a Cu- and Pb-contaminated loess, Environ. Pollut., 333 (2023) 11.

[24] F.L. Cheng, S.H. Guo, G. Li, S. Wang, F.M. Li, B. Wu, The loss of mobile ions and the aggregation of soil colloid: Results of the electrokinetic effect and the cause of process termination, Electrochim. Acta, 258 (2017) 1016-1024.

[25] H.H. Lee, J.W. Yang, A new method to control electrolytes pH by circulation system in electrokinetic soil remediation, J. Hazard. Mater., 77 (2000) 227-240.

[26] J.Y. Park, J.H. Kim, Switching effects of electrode polarity and introduction direction of reagents in electrokinetic-Fenton process with anionic surfactant for remediating iron-rich soil

Journal Pre-proof

548 contaminated with phenanthrene, Electrochim. Acta, 56 (2011) 8094-8100.

549 [27] O.M. Boulakradeche, O. Merdoud, D.E. Akretche, Enhancement of electrokinetic remediation

550 of lead and copper contaminated soil by combination of multiple modified electrolyte conditioning

551 techniques, Environ. Eng. Res., 27 (2022) 11.

552 [28] S. Barba, J. Villaseñor, M.A. Rodrigo, P. Cañizares, Effect of the polarity reversal frequency in

553 the electrokinetic-biological remediation of oxyfluorfen polluted soil, Chemosphere, 177 (2017)

554 120-127.

555 [29] E. Mena, J. Villaseñor, M.A. Rodrigo, P. Cañizares, Electrokinetic remediation of soil polluted

556 with insoluble organics using biological permeable reactive barriers: Effect of periodic polarity

557 reversal and voltage gradient, Chem. Eng. J., 299 (2016) 30-36.

558 [30] Z. Feng, Z. Yang, S. Yang, H.X. Xiong, Y. Ning, C.X. Wang, Y.L. Li, Current status and future

559 challenges of chlorobenzenes pollution in soil and groundwater (CBsPSG) in the twenty-first

560 century: a bibliometric analysis, Environmental Science and Pollution Research, 30 (2023) 111748-

561 111765.

562 [31] Z. Kurt, J.C. Spain, Biodegradation of Chlorobenzene, 1,2-Dichlorobenzene, and 1,4-

563 Dichlorobenzene in the Vadose Zone, Environ. Sci. Technol., 47 (2013) 6846-6854.

564 [32] Y. Lu, Z.F. Chen, Y.J. Chen, Y.Z. Xu, Y.Y. Chen, X.X. Dai, L. Yao, Z.H. Qi, Z.W. Cai,

565 Distribution and risk assessment of hexachlorobutadiene, pentachloroanisole, and chlorobenzenes

566 in sediment and wild fish from a region affected by industrial and agricultural activities in South

567 China, J. Hazard. Mater., 417 (2021) 8.

568 [33] W.J. Qiao, F. Luo, L. Lomheim, E.E. Mack, S.J. Ye, J.C. Wu, E.A. Edwards, Natural

569 Attenuation and Anaerobic Benzene Detoxification Processes at a Chlorobenzene-Contaminated

570 Industrial Site Inferred from Field Investigations and Microcosm Studies, Environ. Sci. Technol.,
571 52 (2018) 22-31.
572 [34] S.C. Yuan, H. Hu, H. Huang, Z.M. Chen, J.X. Chen, M. Zhang, K.P. Li, T. Zhou, R.B. Lv,
573 Research on the reaction path of chlorobenzene oxidation by electrochemical-sodium persulfate
574 system, Journal of Cleaner Production, 420 (2023) 13.
575 [35] P.R. Hegele, K.G. Mumford, Gas production and transport during bench-scale electrical
576 resistance heating of water and trichloroethene, J. Contam. Hydrol., 165 (2014) 24-36.
577 [36] Z.J. Wang, Z.B. Yang, F. Fagerlund, H. Zhong, R. Hu, A. Niemi, T. Illangasekare, Y.F. Chen,
578 Pore-Scale Mechanisms of Solid Phase Emergence During DNAPL Remediation by Chemical
579 Oxidation, Environ. Sci. Technol., 56 (2022) 11343-11353.
580 [37] D.M. Tuck, G.M. Iversen, W.A. Pirkle, Organic dye effects on dense nonaqueous phase liquids
581 (DNAPL) entry pressure in water saturated porous media, Water Resour. Res., 39 (2003).
582 [38] C. Yang, C. Zhang, F. Liu, J. Dong, Remediation of DNAPL-contaminated heterogeneous
583 aquifers using colloidal biliquid aphron: Multiscale experiments and pore-scale simulations, Journal
584 of Hydrology, 628 (2024) 130532.
585 [39] Z. Geng, D. Zheng, Z. Qi, Q. Xie, G. Li, F. Zhang, Direct current driven persulfate delivery
586 and activation for heterogeneous porous media remediation: Coupling effects of electric-thermal-
587 chemical-flow fields, J. Hazard. Mater., 479 (2024) 135743.
588 [40] D.D. Wen, X.P. Guo, R.B. Fu, Inhibition characteristics of the electrokinetic removal of
589 inorganic contaminants from soil due to evolution of the acidic and alkaline fronts, Process Saf.
590 Environ. Prot., 155 (2021) 12.
591 [41] K. Kamran, M. van Soestbergen, H.P. Huinink, L. Pel, Inhibition of electrokinetic ion transport

Journal Pre-proof

592 in porous materials due to potential drops induced by electrolysis, Electrochim. Acta, 78 (2012) 229-
593 235.
594 [42] R. Sprocati, A. Gallo, R. Sethi, M. Rolle, Electrokinetic Delivery of Reactants: Pore Water
595 Chemistry Controls Transport, Mixing, and Degradation, Environ. Sci. Technol., 55 (2021) 719-729.
596 [43] C. Zhao, K.G. Mumford, B.H. Kueper, Laboratory study of non-aqueous phase liquid and water
597 co-boiling during thermal treatment, J Contam Hydrol, 164 (2014) 49-58.
598 [44] Z.S. Yang, C.L. Wei, X. Song, X. Liu, Z.W. Tang, P. Liu, Y.X. Wei, Thermal conductive heating
599 coupled with in situ chemical oxidation for soil and groundwater remediation: A quantitative
600 assessment for sustainability, Journal of Cleaner Production, 423 (2023) 10.
601

Journal Pre-proof

Journal Pre-proof

Highlights

- Regulating ion migration pathways effectively improved the PDC heating process.
- Hydraulic circulation and polarity reversal were effective ion control measures.
- Average temperature and uniformity greatly improved compared to unregulated system.
- DNAPL removal efficiency increased by 19.8%~37.8%, with lower energy consumption.

Journal Pre-proof

Journal Pre-proof

Declaration of interests

☒ The authors declare that they have no known competing financial interests or personal relationships that could have appeared to influence the work reported in this paper.

☐ The authors declare the following financial interests/personal relationships which may be considered as potential competing interests:

Journal Pre-proof